BASIC SCIENCE

Nanomedicine: Nanotechnology, Biology, and Medicine
14 (2018) 661–672

Original Article

nanomedjournal.com

Uptake and intracellular fate of cholera toxin subunit b-modified mesoporous silica nanoparticle-supported lipid bilayers (aka protocells) in motoneurons

Maria A. Gonzalez Porras, PhD[a], Paul Durfee, PhD[c], Sebastian Giambini[a], Gary C. Sieck, PhD[a,b], C. Jeffrey Brinker, PhD[c,d,e,f], Carlos B. Mantilla, MD, PhD[a,b,*]

[a]*Department of Physiology & Biomedical Engineering, Mayo Clinic, Rochester, MN, United States*
[b]*Department of Anesthesiology and Perioperative Medicine, Mayo Clinic, Rochester, MN, United States*
[c]*Center for Micro-Engineered Materials, University of New, Mexico*
[d]*Department of Chemical and Biological Engineering University of New, Mexico*
[e]*Department of Molecular Genetics and Microbiology University of New, Mexico*
[f]*Self-Assembled Materials Department, Sandia National Laboratories, Albuquerque, New, Mexico*

Received 8 June 2017; accepted 2 January 2018

Abstract

Cholera toxin B (CTB) modified mesoporous silica nanoparticle supported lipid bilayers (CTB-protocells) are a promising, customizable approach for targeting therapeutic cargo to motoneurons. In the present study, the endocytic mechanism and intracellular fate of CTB-protocells in motoneurons were examined to provide information for the development of therapeutic application and cargo delivery. Pharmacological inhibitors elucidated CTB-protocells endocytosis to be dependent on the integrity of lipid rafts and macropinocytosis. Using immunofluorescence techniques, live confocal and transmission electron microscopy, CTB-protocells were primarily found in the cytosol, membrane lipid domains and Golgi. There was no difference in the amount of motoneuron activity dependent uptake of CTB-protocells in neuromuscular junctions, consistent with clathrin activation at the axon terminals during low frequency activity. In conclusion, CTB-protocells uptake is mediated principally by lipid rafts and macropinocytosis. Once internalized, CTB-protocells escape lysosomal degradation, and engage biological pathways that are not readily accessible by untargeted delivery methods.

Key words: Mesoporous silica nanoparticles; Motoneuron; Neuromuscular junction; Cholera toxin subunit B; Macropinocytosis; Lipid raft endocytosis

Protocells represent an emerging class of bionanomaterials with exceptional therapeutic potential.[1,2] Protocells consist of a mesoporous silica nanoparticle core (MSNP) encapsulated by a supported lipid bilayer.[3,4] As a drug delivery system, the cargo loading, bio-functionality and bio-compatibility of protocells can be independently modified by engineering pore size, and surface chemistry including the characteristics of the supported lipid bilayer.[1,2] We previously showed that protocells can be engineered to specifically target motoneurons by modifying the lipid bilayer with cholera toxin subunit B (CTB-protocell), the atoxic subunit of cholera toxin that binds the ganglioside GM1 present in neuronal membranes, and successfully deliver small molecule cargo.[5] Knowledge of the biological mechanism(s) governing cellular uptake and trafficking after CTB-protocell

There are no known conflicts of interest associated with this publication and there has been no significant support for this work that could have influenced its outcome. This project was supported by internal funding from the Mayo Foundation. CJB acknowledges support from the Sandia National Laboratories (SNL) Laboratory-Directed Research Development program and DTRA project IAA DTRA1002720595. SNL is a multi-mission laboratory managed and operated by National Technology and Engineering Solutions of Sandia, owned subsidiary of Honey-well International, Inc., for the U.S. Department of Energy's National Nuclear Security Administration under contract DE-NA-0003525.

*Corresponding author at: Joseph 4-184 W, St Marys Hospital, Mayo Clinic, Rochester, MN 55905.
E-mail address: mantilla.carlos@mayo.edu (C.B. Mantilla).

https://doi.org/10.1016/j.nano.2018.01.002
1549-9634/

internalization in motoneuron-targeted delivery is important to inform selection of appropriate protocell cargo. Mechanisms responsible for cellular uptake, e.g., endocytosis, also determine intracellular pathways involved in trafficking of internalized moieties and these effects depend on cell type.[6] Despite the importance of motoneurons to human health and disease, the control of neuronal membrane dynamics and the molecular basis of specific endocytic events with retrograde transport pathways remain largely unknown. It is likely that therapeutic efficacy of novel drug delivery systems will depend on intracellular delivery to specialized organelles, and thus, understanding the uptake and trafficking of nanoparticles is essential to inform drug cargo and their therapeutic application.

Nanoparticle uptake and intracellular trafficking depend on various physicochemical characteristics including particle size, shape, density, and surface chemistry and the endocytic pathways in a given cell type.[7,8] Nanoparticles can be internalized in cells by endocytosis, which involves the expenditure of metabolic energy, the movement and fusion of membranes and the displacement of cytoplasm in a complex series of events.[9] Nanoparticles can also translocate through a membrane passively by deformation of membrane lipids.[10] Since CTB internalization is associated with lipid raft endocytosis because of GM1 binding to rafts[11] and the size of raft domains is highly variable, CTB-protocell internalization may be limited to a subset of lipid rafts that include larger transient confinement domains (up to 700 nm in dimension).[12] Macropinocytosis reflects the formation of big endocytic vesicles that sequester a large amount of fluid-phase contents. Among cells and in neurons, macropinocytosis is highly present due to its importance in cell-to-cell communication.[13] In various cells, macropinocytosis can be triggered by a variety of factors including nanoparticles.[10]

Neurons undergo substantial membrane cycling at synapses in an activity-dependent fashion and membrane uptake varies depending on the rate of stimulation such that synaptic membrane recycling during physiological rates of activation primarily reflects clathrin-mediated endocytosis rather than macropinocytosis or other form of bulk membrane retrieval that has been reported during maximal (albeit non-physiological) activation.[14,15] We hypothesized that CTB-protocell uptake in motoneurons is mediated by lipid raft endocytosis and macropinocytosis; and uptake is not affected by activity at the neuromuscular junction (NMJ). These internalization pathways are commonly associated with retrograde intracellular trafficking to the Golgi and endoplasmic reticulum, although transfer to endolysosomal compartments for ultimate degradation is also possible.[8] Accordingly, we also hypothesized that after internalization CTB-protocells can escape the endo-lysosomal pathway for degradation and become available to the cell.

Methods

All procedures involving animals were approved by the Institutional Animal Care and Use Committee at Mayo Clinic and in accordance with humane treatment guidelines by the American Veterinary Medical Association. Adult male Sprague–Dawley rats (initial body weight ~300 g) were used in each of the animal experiments.

Preparation of mesoporous silica-supported lipid bilayer nanoparticles (protocells)

MSNPs with spherical shape and dendritic 5 nm diameter pore were synthesized via a base-catalyzed solution-based surfactant-directed self-assembly method, adapted from a published biphase synthesis method,[16–18] and fusion of liposomes to MSNPs (protocell assembly) as previously described.[5,18] Lipid films formed by drying cholesterol, 1,2-distearoyl-sn-glycero-3-phosphocholine and 1,2-distearoyl-sn-glycero-3-phosphoethanolamine-N-[amino(-polyethyleneglycol)-2000] phospholipids (Avanti Polar Lipids, Birmingham, AL) were added to MSNPs dissolved in 0.5× PBS. CTB was conjugated to the protocells using the NeutrAvidin/biotin conjugation strategy described before.[5,18]

Motoneuron cell culture and CTB-protocell treatment

NSC-34 motoneuron-like cells were propagated in 75 cm^2 flasks in Dulbecco's Modified Eagle Medium/Nutrient Mixture F-12, with GlutaMAX (ThermoFisher Scientific; Waltham, MA) supplemented with 10% fetal bovine serum and 2% Penicillin–Streptomycin. Cells were differentiated for 24 h with serum-deprived media.

Assessment of energy dependent uptake of CTB-protocells

Cells were incubated with CTB-protocells for 1 h at 37 or 4 °C, washed and fixed in 4% paraformaldehyde (PFA). Images were obtained with a 60× oil immersion lens (NA 1.2) using a Nikon A1 confocal microscope (Nikon Instruments Inc.) with laser intensity, confocal aperture, and photomultiplier gain kept constant across samples. NIS-Elements software (Nikon) was used for image processing and analysis. Single plane images were acquired in the nuclei midline of differentiated motoneurons and the mean protocell fluorescence per cell was quantified. To confirm the energy dependence in the uptake of CTB-protocells, an ATP depletion assay was conducted using 1 M sodium azide (NaN_3) and 0.6 M of 2-deoxy-D-glucose (Sigma-Aldrich) diluted in glucose free Dulbecco's Modified Eagle Medium for 1 h, as previously described.[19] ATP depleted medium was removed and cells were treated with 50 μg/ml of CTB-protocells diluted in glucose free medium for 1 h. After washes, cells were imaged using the procedure described previously.

Assessment of CTB-protocell internalization

To understand the role of lipid-raft microdomains, cells were incubated with CTB-protocells for 1 h, rinsed with PBS, and incubated with Alexa Fluor 488-labeled CTB (8 μg/ml, ThermoFisher) for 20 min at 37 °C followed by fixation in 4% PFA, and confocal imaging to measure the extent of colocalization. To study the different types of endocytosis, cells were pre-incubated with various endocytic chemical inhibitors for 30 min followed by 1 h of CTB-protocells treatment. 1 mM of methyl-β-cyclodextrin (MβCD) (Sigma-Aldrich) was used to inhibit cholesterol dependent endocytic processes (lipid rafts endocytosis) and 14 μg/ml of amiloride (Sigma-Aldrich) was used to inhibit macropinocytosis. Cellular fluorescence resulting from internalization of CTB-protocells was quantified per cell.

Subcellular localization of CTB-protocells

To examine the position of CTB-protocells relative to the endo-lysosomal pathway, antibodies against: early endosome antigen 1 (EEA1; ThermoFisher) as a marker of early endosomes, and lysosomal-associated membrane protein 1 (LAMP1; Abcam, Cambridge, MA) were used in cells after treatment with CTB-protocells for 1 h, 3 h, 6 h and 24 h. Confocal images were taken (Nikon A1) and quantitative colocalization analysis was performed using the Manders' coefficient (ImageJ). In a second approach, a pulse-chase setup to follow a small window of uptake events was used. Cells were treated with CTB-protocells for 1 h and then placed intro fresh media and imaged at different times (1 h, 3 h, 6 h and 24 h). Cells were incubated before CTB-protocells treatment with 1) LysoTracker® Blue DND-22 (ThermoFisher) for 30 min to stain acidic vacuoles; 2) CellLight® Early Endosomes-GFP, BacMam 2.0, (ThermoFisher) for 24 h to label early endosomes with green fluorescent protein (GFP) in live cells; 3) ER-tracker™ Blue-White DPX (ThermoFisher) to selectively label the ER or 4) BODIPY® TR Ceramide (ThermoFisher) to label the lipid trafficking and Golgi in living cells. Live cells were imaged using an inverted confocal microscope with 60× (NA 1.4) oil-immersion objective. Colocalization with organelles was quantified using the intersection operation of the Elements software, which permits binarization of the intensity field and subsequent pixel intersection. To determine the elimination of CTB-protocells in cells, the fluorescence of rhodamine-labeled protocells was measured up to 5 days post-treatment using a FlexStation 3 microplate reader system (Molecular Devices, Sunnyvale, CA). The elimination half-life was determined using a quadratic equation.

Ultrastructural localization of CTB-protocells

Cells were incubated with CTB-protocells for 1 h, 3 h, 6 h or 24 h and fixed in Trump's fixative (1% glutaraldehyde and 4% formaldehyde in 0.1 M phosphate buffer, pH 7.2). Cells were rinsed in 0.1 M phosphate buffer (pH 7.2), followed by 30 min postfix in phosphate-buffered 1% osmium tetroxide (OsO_4). After rinsing in distilled water, cells were stained with 2% uranyl acetate for 15 min at 60 °C, rinsed, dehydrated in progressively higher concentrations of ethanol and 100% propylene oxide, and embedded in Spurr's resin. Thin (100 nm) sections were obtained using Leica EM UC7 ultramicrotome (Buffalo Grove, IL), then placed on 200 mesh copper grids, and stained with lead citrate. Micrographs were acquired on a JEOL JEM-1400 Transmission Electron Microscope (TEM, Tokyo, Japan) operating at 80 kV.

Activity dependent uptake of CTB-protocells in axon terminals

Uptake of CTB-protocells at NMJs was determined by visualizing changes in CTB-protocell fluorescence intensity, with and without phrenic nerve stimulation.

Diaphragm muscle-phrenic nerve preparation

The midcostal hemidiaphragm and phrenic nerve were rapidly excised and placed in Rees–Simpson solution (in mM: Na^+135, K^+5, Ca^{2+}2, Mg^{2+}1, Cl^-120, HCO^{3-}25) while bubbled with 95% O_2/5% CO_2 at 26 °C. Subsequently, the excised hemidiaphragm-phrenic nerve was stretched to optimal length (1.5× resting length) and mounted on a silico rubber-coated dish (Sylgard DowCorning, Midland, MI).

CTB-protocell treatment and NMJ labeling

In order to label recycling synaptic vesicles as they undergo cycles of exo- and endocytosis, FM1-43 (Ex: 510 nm, Em: 626 nm; Molecular Probes, Eugene, OR) was used. Tissue preparations were incubated in Rees–Simpson solution containing 50 μg/ml CTB-protocells and 5 μM FM1-43. The phrenic nerve was taken into a suction electrode and stimulated using an A-M systems 2100 isolated pulse stimulator at 10 Hz (0.5 ms supramaximal pulses with 67% duty cycle) for 1 h. Following a 15-min wash, acetylcholine receptors at motor end-plates were fluorescently labeled with Alexa Fluor 647-conjugated α-bungarotoxin (Ex: 650, Em: 665 nm) (Invitrogen, Carlsbad, CA) to facilitate visualization of NMJs.

Diaphragm NMJs were visualized using a Nikon C1 confocal microscope with a 40× (NA 0.8) water immersion lens at 3 μm step size with simultaneous three-channel detection. A region of interest (ROI) outlining the motor end-plate of each NMJ was drawn from the maximum intensity projection in Nikon Elements. Within this ROI, the protocell fluorescence intensity was examined in each plane of the z-stack comprising the NMJ. The mean fluorescence intensity for each motor end-plate was measured and the background subtracted.

Neuromuscular transmission measurements

Neuromuscular transmission failure (NMTF) was assessed using a previously described technique.[20,21] Briefly, midcostal diaphragm-phrenic nerve preparations (3-4 mm wide) were pre-incubated with CTB-protocells (50 μg/ml) for 1 h in Rees–Simpson solution. Subsequently, isometric twitch force (P_t) and maximum tetanic force (P_o) were measured for each diaphragm segment. To measure the rate of NMTF, the phrenic nerve was stimulated (0.1-ms pulse at supramaximal intensity) using a suction electrode at 40 Hz in 330-ms duration trains repeated each second for a 2-min period. Every 15 s, direct muscle stimulation (via plate electrodes; 1-ms supramaximal pulses at 40 Hz in 330-ms trains) was superimposed. The relative contribution of NMTF to muscle fatigue was estimated by the equation: $NMTF = (F - MF)/(1 - MF)$, where F is a percent decrement in force during repetitive nerve stimulation, and MF is the percent force decrement during direct muscle stimulation.

In vivo CTB-protocell treatment by intrapleural injections

Awake animals were lightly restrained ($n = 3$), and a 50-μl Hamilton syringe was used to intrapleurally inject 50 μl of 1 μg/μl CTB-protocells in the fifth intercostal space via transcutaneous injection into the thoracic cavity (5-7 mm deep, from skin), as in previous studies.[22] Animals were monitored closely for signs of respiratory compromise such as unintentional pneumothorax, but none were evident.

CTB-protocell imaging

At 24 h post-injection, rats were euthanized, and following transcardial fixation, a 5-10 mm segment of the phrenic nerve (proximal to the diaphragm) was dissected, and the epineurium was removed and immersed in 24% sucrose in PBS for cryoprotection. Nerves were incubated in anti-neurofilament (Millipore Sigma; Burlington, MA) to label axons, followed by appropriate secondary antibody. Nerve segments were treated

with graded alcohols and xylene, and coverslipped with DPX mountant (Fluka; Sigma-Aldrich, St. Louis, MO). Confocal fluorescence imaging of the nerve segment was performed using a Nikon C1 confocal microscope with 20× 0.8 NA oil immersion lens at 0.8 μm step size. Confocal stacks of optical sections were used to generate 3D reconstructions using Nikon Elements.

Statistical analyses

All statistical evaluations were performed using standard statistical software (JMP 10.0, SAS Institute Inc., Cary, NC). Differences between treatment groups were examined using one-way analysis of variance, followed by Tukey–Kramer HSD test when appropriate. Statistical significance was established at the $P < 0.05$ level. All experimental data are presented as mean ± SE, unless otherwise specified.

Results

CTB-protocell uptake in motoneurons is energy dependent

Several proteins and enzymes are sensitive to temperature; thus, active processes are decreased by lowered temperatures.[23] CTB-protocell uptake in motoneurons significantly decreased by 54% at 4 °C compared to 37 °C (Figure 1).

Energy dependency in the process of CTB-protocell internalization was corroborated by cellular ATP pool depletion. ATP depletion resulted in characteristic cell shape changes observed by confocal images of motoneuron-like cells. These findings are consistent with evidence that NaN_3 can disintegrate the actin cytoskeleton and destroy microfilament bundles.[24] ATP depletion significantly reduced the uptake of CTB-protocells in motoneuron-like cells after 1 h (59% reduction). Taken together, these results indicate that CTB-protocells are internalized into motoneurons via an energy dependent endocytosis mechanism.

CTB-protocell uptake in motoneurons is mediated by lipid rafts and macropinocytosis

Confocal microscopy confirmed that CTB-protocells also follow the lipid raft pathway previously reported for CTB.[11] 50% of CTB-protocells co-localized with CTB at 1 h and 3 h of incubation (Figure 2), suggesting that lipid rafts play a major role in CTB-protocell uptake but are not the only endocytic mechanism.

Motoneuron-like cells were incubated with two different endocytic inhibitors for 30 min before treatment with CTB-protocells (Figure 3). Following pretreatment with amiloride, (inhibitor of macropinocytosis),[25] CTB-protocell uptake decreased ~60% after 1 h of treatment. A similar inhibition was obtained by pre-treatment with MβCD (inhibitor of lipid rafts endocytosis).[26] In the presence of both amiloride and MβCD, uptake of CTB-protocells was completely abolished, confirming the role of macropinocytosis and lipid raft pathways as the main endocytosis mechanisms in motoneurons. Importantly, uptake of transferrin, one of the best-characterized clathrin-dependent cargoes,[27] was unimpaired after amiloride and MβCD endocytosis inhibitor co-treatment, verifying cell viability and effective endocytosis via a different mechanism.

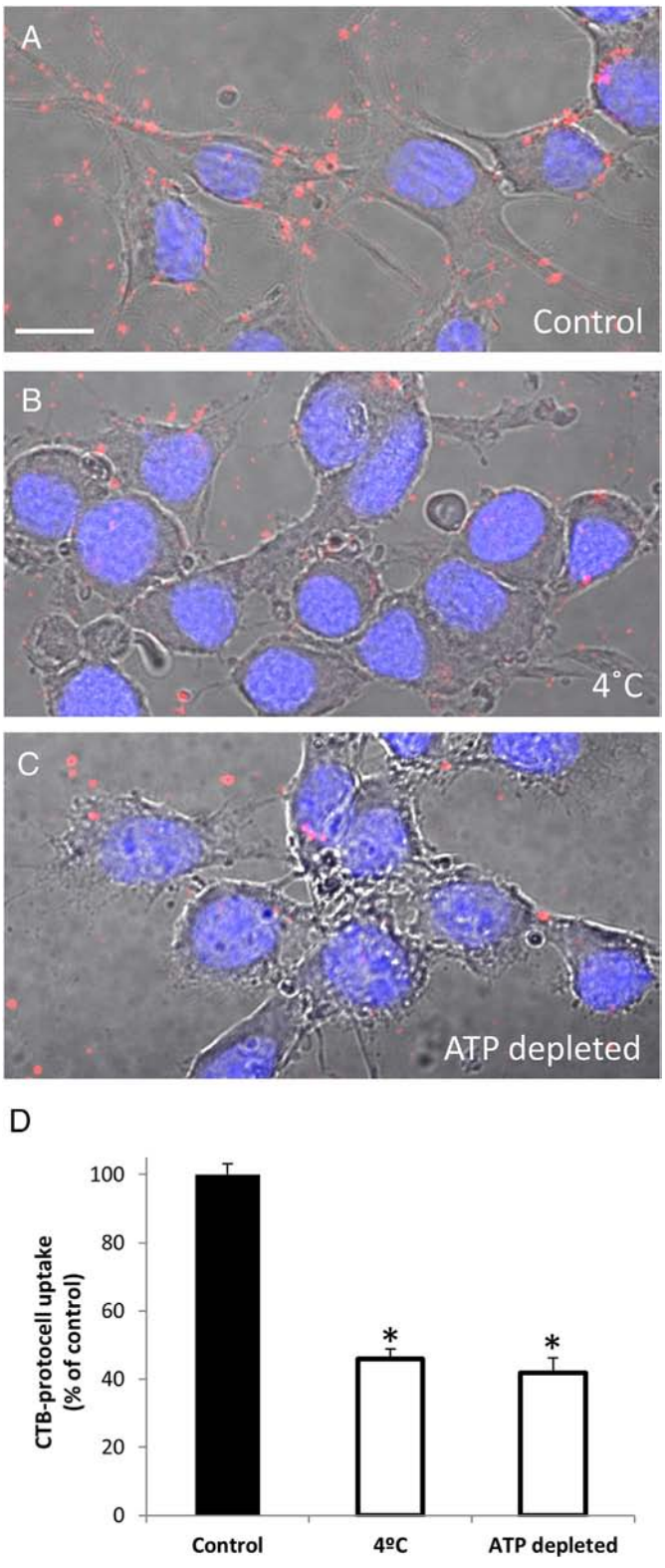

Figure 1. Uptake of CTB-protocells in NSC-34 motoneuron-like cells. (**A-C**) Representative images of cells treated with CTB-protocells for 1 h at 37 °C (**A**), 4 °C (**B**) or following ATP depletion with NaN_3 (1 M) and 2-deoxy-D-glucose (0.6 M) (**C**). Bar, 10 μm. (**D**) Summary of intracellular CTB-protocell uptake (relative to control; n ≥ 100 cells from three independent experiments). *, $P < 0.05$ (ANOVA, $F_{2,497} = 96.11$, $P < 0.001$; *post-hoc* Tukey–Kramer).

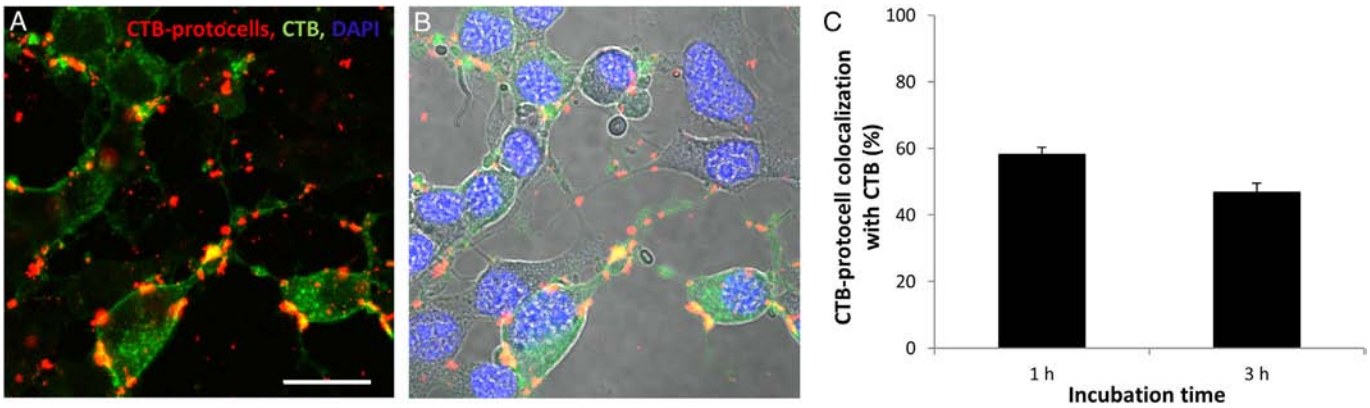

Figure 2. Intracellular uptake of CTB or CTB-protocells by NSC-34 motoneuron-like cells. (**A** and **B**) Representative confocal image (**A**) and superimposed brightfield image (**B**) of CTB-protocells (red), CTB (green), colocalization (yellow) with nuclear stain (DAPI, blue). Bar, 10 mm. (**C**) Proportion of intracellular CTB-protocells displaying colocalization with CTB following 1 and 3 h incubation (n ≥ 75 cells from three independent experiments). CTB-protocells show uptake via pathways shared with CTB (i.e., lipid rafts) but this is limited to 50%-60% of total uptake.

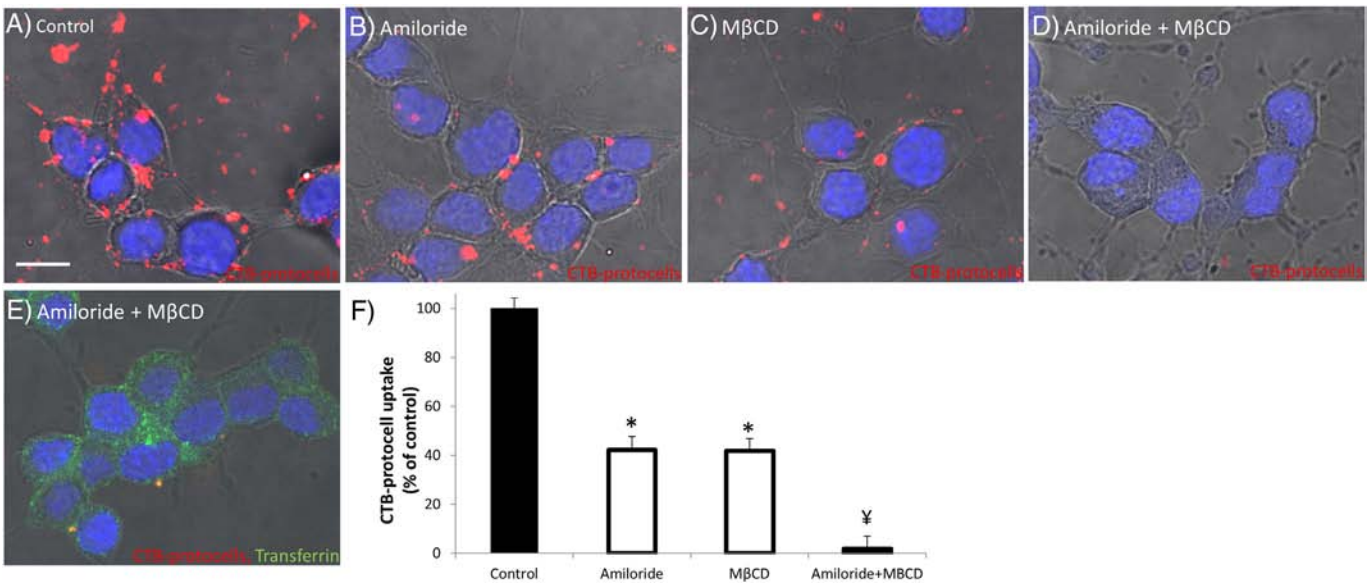

Figure 3. Uptake of CTB-protocells in NSC-34 motoneuron-like cells treated with endocytosis inhibitors. (**A-E**) Representative images of cells incubated with CTB-protocells and (**A**) vehicle, (**B**) amiloride (macropinocytosis inhibitor), (**C**) MβCD (lipid raft endocytosis inhibitor), (**D**) both amiloride and MβCD and (**E**) transferrin plus amiloride and MβCD. Transferrin endocytosis (clathrin-mediated) is evident despite amiloride and MβCD treatment. Bar, 10 μm. (**F**) Summary of intracellular CTB-protocell uptake (relative to vehicle control; $n \geq 80$ cells from three independent experiments). *¥, $P < 0.05$ (ANOVA, $F_{3,395} = 76.48$, $P < 0.001$; post hoc Tukey–Kramer).

In TEM images, membrane ruffling (extensions) was evident engulfing large amounts of CTB-protocells (Figure 4), consistent with macropinocytosis.[28] Lipid raft microdomains, defined by electron dense staining with OsO_4,[29] displayed higher CTB-protocell association than other membrane portions. These imaging results are consistent with confocal imaging studies indicating endocytosis of CTB-protocells in motoneurons is mainly mediated by two mechanisms: lipid rafts and macropinocytosis.

CTB-protocells avoid endolysosomal pathways in motoneurons

Colocalization of CTB-protocells under conditions where cells were continuously incubated (no change in medium) with CTB-protocells (50 μg/ml), was studied. Minimal colocalization (~10%) of CTB-protocells with protein markers for early endosomes (EEA1) or lysosomes (LAMP1) was evident (Table 1), and this level of colocalization was unchanged up to 24 h. In addition, a pulse-chase setup was used to investigate whether continuous exposure to CTB-protocells impacted uptake. Motoneuron-like cells were incubated with CTB-protocells for 1 h at a lower concentration (20 μg/ml) in order to facilitate tracing intracellular CTB-protocells. Single confocal plane images at the mid-nuclear region were superimposed to brightfield images for these analyses (Figure 5). Colocalization of CTB-protocells with the lysosomal stain LysoTracker was less than 20% at all time points. Colocalization with early endosomes labeled by GFP was

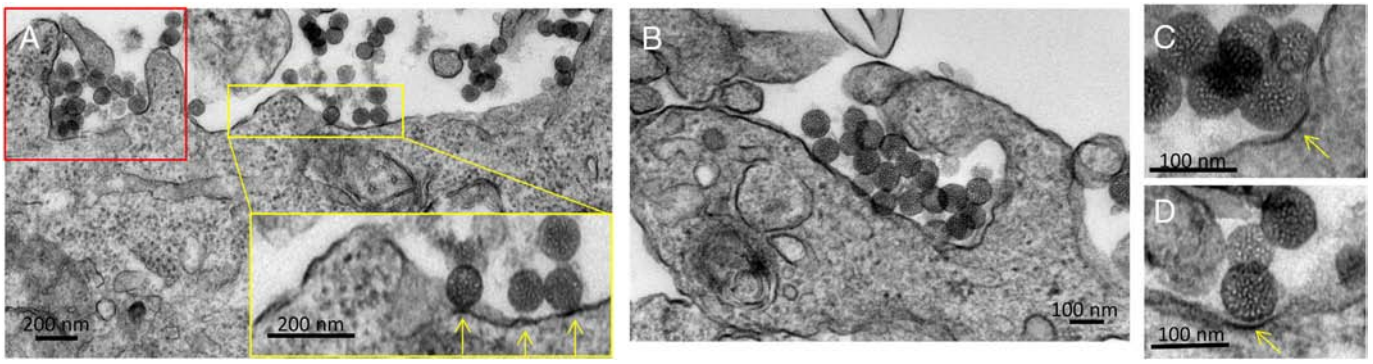

Figure 4. TEM images of NSC-34 motoneuron-like cells incubated with CTB-protocells for 3 h. Uptake of CTB-protocells via macropinocytosis is evident by membrane ruffling (membrane extensions) around CTB-protocells (red box in (**A**), and (**B**)). Association of CTB-protocells with lipid microdomains (membrane sections with increased electron density, arrows in yellow box, inset in (**A**) and (**C**)). Bar, 200 nm in (**A**), 100 nm in (**B**) and 50 nm in (**C-D**).

Table 1
Percent colocalization based on Mander's coefficient.

Time	*Endosomes*	*Lysosomes*
1 h	6.0 ± 1.5%	2.7 ± 1.8%
3 h	10.6 ± 1.2%	9.3 ± 0.9%
6 h	9.6 ± 2.1%	11.3 ± 1.0%
24 h	9.0 ± 2.06%	7.1 ± 0.9%

n = ~300 cells from 2 independent experiments.

also lower than 20% until 6 h and increased to ~30% at 24 h. Taken together, these data indicate that the majority of CTB-protocells do not follow the typical endolysosomal pathway for degradation.

The localization of CTB-protocells in TEM images of motoneuron-like cells collected after continuous treatment is consistent with the results of the confocal studies. At all-time points, CTB-protocells were visualized primarily as individual particles in small membrane bound compartments or in the cytosol (Figure 6). There was scant evidence of CTB-protocells inside larger vesicle compartments such as late endosomes or lysosomes.

CTB-protocells are primarily found in the cytosol and membranous lipid domains in motoneurons

Using a similar pulse-chase setup experiment, colocalization of CTB-protocells with the ER (stained with ErTracker) or lipid-driven membrane domains including the Golgi apparatus (stained with Bodipy) was evaluated (Figure 5). Colocalization of CTB-protocells differed over time across intracellular organelles with greater CTB-protocell localization in the Golgi across time and increasing in endosomes by 24 h. These results indicate that CTB-protocells are directed to the Golgi apparatus as a major membrane sorting station, consistent with previous reports for the trafficking of compounds internalized via lipid raft endocytosis.[11]

Intracellular CTB-protocell fluorescence remained mostly unchanged between 1 h and 24 h of incubation, with a small decrease in fluorescence by 6 h. A similar trend was evident for Golgi colocalization. Results of fluorescence measurements over time showed that the half-life of CTB-protocells in motoneurons is 2.6 ± 0.2 days, indicating a slow exocytosis process consistent with the intracellular pathways followed after lipid raft endocytosis and macropinocytosis (Figure S1), which is expected to be accompanied by protocell degradation via hydrolysis of the MSNP core to form non-toxic silicic acid by-products.[30] TEM images confirmed the confocal imaging data and for up to 24 h of incubation, CTB-protocells were found inside cisternae structures consistent with Golgi or other lipid-driven membrane domains in proximity to nuclei (Figure 6).

CTB-protocell uptake at axon terminals is not influenced by electrical stimulation

Good visualization of both presynaptic and postsynaptic structures was evident (Figure 7). FM1-43 uptake only occurred with repeated nerve stimulation. In the absence of stimulation, uptake was minimal. CTB-protocell fluorescence showed larger punctate structures, suggesting their presence in structures other than synaptic vesicles such as macropinosomes.[31] Indeed, these punctate structures were visualized at NMJs of hemi-diaphragms with and without phrenic nerve stimulation and CTB-protocell uptake did not change with phrenic nerve stimulation at the low, physiological rate tested (10 Hz).

CTB-protocell uptake at motoneuron axon terminals does not impair synaptic transmission

The effects of CTB-protocell treatment on synaptic transmission, measured as the extent of NMTF, are presented in Table 2. There was no difference in the contribution of NMTF to muscle fatigue with repetitive stimulation between control, untreated and CTB-protocell treated diaphragm muscle-phrenic nerve preparations. There was also no change in contractile and fatigue properties of the diaphragm muscle across groups.

CTB-protocell fluorescence is evident in the phrenic nerve after in vivo intrapleural injection

Intrapleural CTB was previously shown to label phrenic motoneurons in the cervical spinal cord by retrograde transport.[22] As proof of concept, the presence of CTB-protocells was evaluated in the phrenic nerve at 24 h after intrapleural administration. CTB-protocell fluorescence was evident in all phrenic nerve whole mounts (Figure 8; $n = 3$). In 3D reconstructions of the phrenic

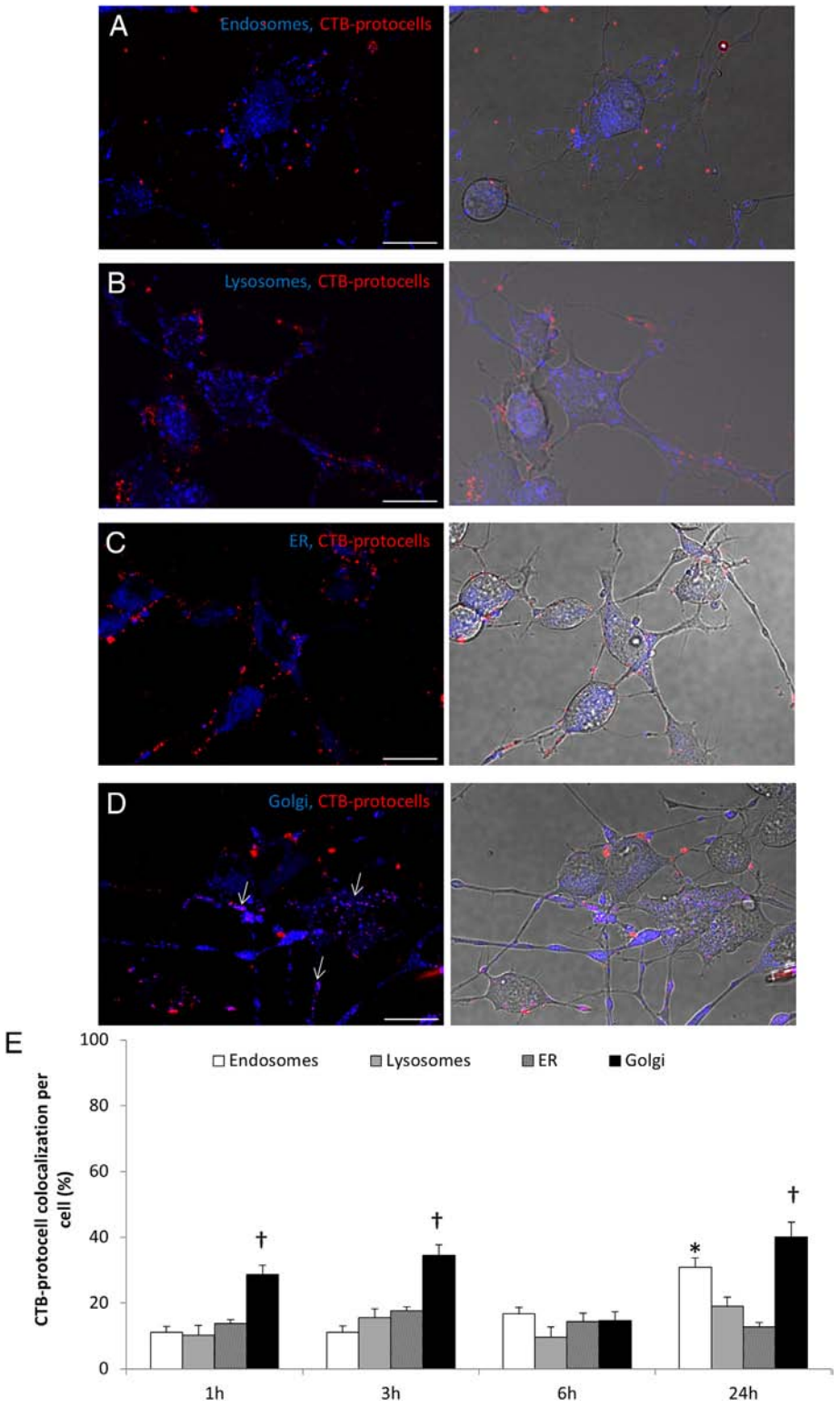

Figure 5. Distribution of CTB-protocells across intracellular NSC-34 motoneuron-like cells. (**A-D**) Representative confocal (left) and superimposed brightfield images (right) after 1 h treatment with CTB-protocells and organelle labeling for lysosomes (**A**), endosomes (**B**), ER (**C**) or Golgi (**D**). Bar, 20 μm. (**E**) Summary of CTB-protocell colocalization with different organelles (two-way ANOVA, $F_{15,929} = 10.04$, $P < 0.0001$; post hoc Tukey–Kramer, $P < 0.05$; *, different from other time points; †, different from other organelles at same time point). $n \geq 75$ cells from three independent experiments.

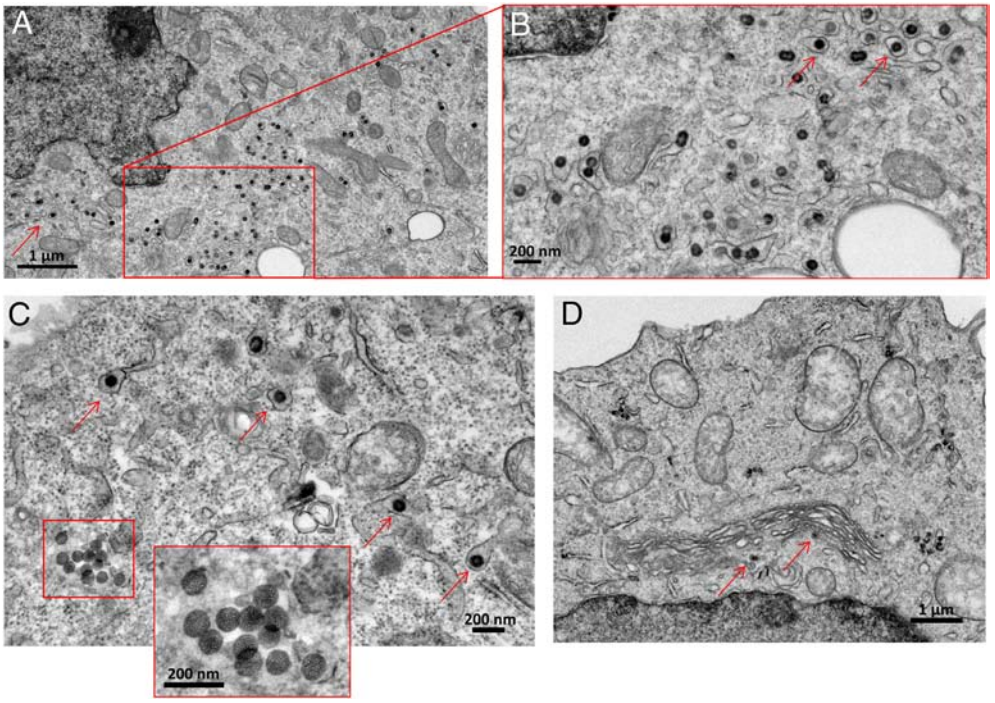

Figure 6. TEM images of intracellular CTB-protocells in NSC-34 motoneuron-like cells. Note CTB-protocells are visualized as individual particles in the cytosol (red boxes and inset in **A** (**B**) and **C**) as well as small membrane bound compartments (arrows, consistent with early endosomes or Golgi). Also note lack of localization in larger vesicle compartments (e.g., late endosomes or lysosomes).

nerve, CTB-protocells were closely associated with axonal neurofilament immunoreactivity throughout the entire thickness of the phrenic nerve, indicating uptake and retrograde transport by motoneuron axons in vivo.

Discussion

CTB-protocells represent a novel drug delivery system to motoneurons that can engage biological retrograde pathways not easily reached with untargeted delivery methods. Understanding the mechanisms responsible for cellular uptake and the associated intracellular pathways involved in trafficking of CTB-protocells provides novel insight into the selection of drugs for therapeutic delivery to motoneurons (both in heath and disease). The cytosolic availability of CTB-protocells and avoidance of lysosomal degradation fulfill an important medical need of targeted vehicles that can load different cargoes for the treatment of neuromuscular disorders, given that current treatments are limited and hindered by bioavailability and off-target effects.[32,33] The proof-of-concept information showing that intrapleural (and thus possibly systemic) administration of CTB-protocells harnesses retrograde axonal transport mechanisms in motoneurons provides exciting new directions for CTB-protocells as a drug delivery system.

Endocytosis of CTB-protocells in motoneurons

Endocytosis occurs via various mechanisms and in motoneurons can take place at the dendrites, cell bodies, and axons. We examined endocytosis both in cultured NSC-34 motoneuron-like cells and at NMJs of rat diaphragm muscle-phrenic nerve preparations. The NSC-34 cells share endocytosis mechanisms with motoneurons *in vivo,*[34,35] and in a previous study, NSC-34 cells have been useful in understanding receptor trafficking within motoneurons.[35] Furthermore, GM1 ganglioside is expressed by NSC-34 cells and motoneurons *in vivo,*[5] and thus NSC-34 cells are ideal to study the internalization and intracellular pathways of CTB and CTB-protocells. CTB-modified protocells were previously reported to show uptake by cultured motoneurons and axon terminals in a selective manner, compared to unmodified protocells.[5] Consistent with the targeting to motoneurons following modification with CTB, CTB-protocells showed extensive, but not exclusive, colocalization with CTB. Previous studies also support the targeting to motoneurons with systemic CTB administration.[36]

Pathways involved in endocytosis are energy dependent. Indeed, we found generally similar effects on CTB-protocell uptake in studies conducted at low temperature and following ATP depletion (~60% decrease). Low levels of residual nanoparticle uptake are still observed at temperatures and chemical exposures supporting cell viability.[37,38]

CTB uptake by cells is known to reflect interactions with lipid domains rich in GM1 gangliosides.[39] Consistent with the CTB internalization pathway, inhibition of lipid rafts endocytosis by MβCD decreased the CTB-protocell uptake in 40%. MβCD is a cyclic oligomer of glucopyranoside that inhibits cholesterol-dependent endocytic processes by reversible extracting the steroid out of the plasma membrane.[40] The colocalization of some CTB-protocells with CTB and the inhibition of half of the CTB-protocell uptake by disruptors of lipid rafts, confirm that indeed some CTB-protocells follow the CTB endocytic

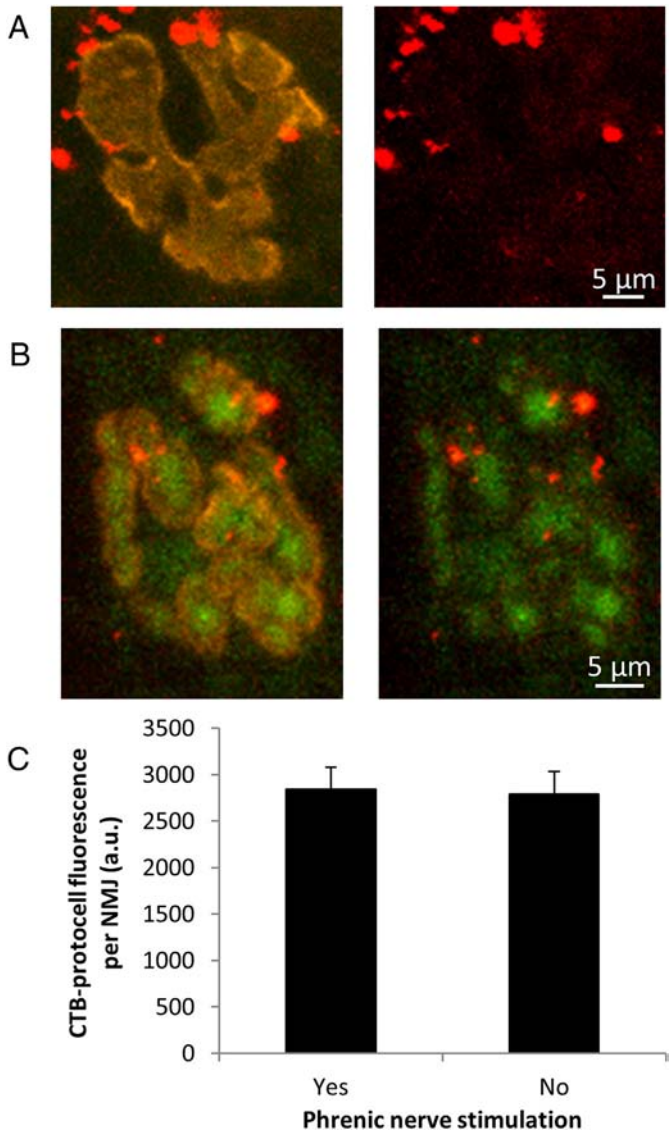

Figure 7. Representative maximum intensity projection confocal micrographs of diaphragm NMJs. Diaphragm muscle-phrenic nerve preparations were incubated (**A**) in the absence of electrical stimulation and (**B**) with 1 h of repetitive electrical nerve stimulation (10 Hz, 0.1 ms, 300 ms trains repeated every s). (**C**) Average CTB-protocell fluorescence per NMJ (n = 90 NMJs per stimulation group from 3 preparations for each condition).

pathway, but also imply the existence of another endocytic mechanism. Given that macropinocytosis a highly present process in neurons,[41] it is more likely that other particles such as viruses and nanoparticles, hijack the machinery involved in macropinocytosis to gain cell entry.[42,43] Inhibition of macropinocytosis with amiloride (an inhibitor of Na/H exchange at the cell surface),[44] decreased the uptake of CTB-protocells by ~60%. Furthermore, co-incubation of CTB-protocells with both inhibitors (amiloride and MβCD) completely blocked the CTB-protocell uptake, indicating that CTB-protocells are using lipid rafts and macropinocytosis as a primary entry mechanism and its uptake is not occurring by passive mechanisms. Cell viability after chemical

Table 2
Neuromuscular transmission failure (NMTF) and isometric contractile and fatigue properties following CTB-protocell treatment.

Group	NMTF (%)	Specific P_t ($N*cm^{-2}$)	Specific P_o ($N*cm^{-2}$)	P_t/P_o
Control	58.4 ± 8.4	5.61 ± 0.46	17.1 ± 1.03	0.33 ± 0.02
CTB-protocells	58.3 ± 8.4	5.54 ± 0.46	17.4 ± 1.03	0.32 ± 0.02

Diaphragm muscle-phrenic nerve preparations and diaphragm muscle strips were obtained from n = 3 animals per group. Data are mean ± SE.

inhibitor treatments was confirmed by un-impairment of transferrin endocytosis, a molecule internalized by clathrin endocytosis.

Although the use of chemical inhibitors reveals molecular components required for CTB-protocell internalization, they could have indirect effects that may influence another process in the cell.[45] To overcome these limitations, TEM images were used to observe how CTB-protocells interact with motoneuron membranes. Images showed distinctive characteristics of CTB-protocells being endocytosed by lipid rafts (CTB-protocells interaction with membrane electron dense staining) and macropinocytosis (membrane ruffling engulfing a large amount of CTB-protocells).[29,46]

Intracellular trafficking pathways in motoneurons

Intracellular pathways are dictated by the endocytosis mechanisms.[6] After lipid raft endocytosis, the CTB intracellular distribution is known to follow a retrograde pathway and travels from an early endosome through the trans-Golgi network.[11] The pathway of macropinosomes depends on the cell type. For example in macrophages, macropinosomes become acidified and then completely merge into the lysosomal compartment,[47] while in other cells although the pH decreases, macropinosomes do not fuse into lysosomes and can become "leaky" vesicles.[48] In a continuous exposure of CTB-protocells to motoneuron-like cells up to 24 h, there was minimal colocalization of CTB-protocells with endosomes (EEA1) and lysosomes (LAMP1). Since fluorescent colocalization studies using confocal microscopy have limited spatial resolution, we also used TEM images to confirm intracellular CTB-location. TEM images did not show CTB-protocells in double membrane vesicles, usually recognized as lysosomes or late endosomes. In addition, to analyze a small window of uptake events (1 h) instead of continuous treatment, we used a pulse-chase setup yielding similar consistent results in terms of CTB-protocell subcellular localization. The general larger colocalization with membranous lipid domains and the Golgi apparatus observed in confocal and TEM images compared to other organelles is consistent with its role as a membrane sorting station of lipid raft microdomains.[49] In neurons, the Golgi is not only important in the trafficking of ion channels, receptors, and other signaling molecules, but also mediates transport of exogenous molecules by retrograde and trans-synaptic pathways.[50] Lipid raft endocytosis is usually a nonacidic and nondigestive route of internalization,[51] and lipid binding toxins, such as CTB, are transported via the Golgi to the endoplasmic reticulum.[11] Therefore, it is most likely that the CTB-protocells internalized through lipid raft microdomains would travel to the Golgi complex. Consistent with CTB-protocells taking a retrograde pathway, CTB-protocells show promise as a platform

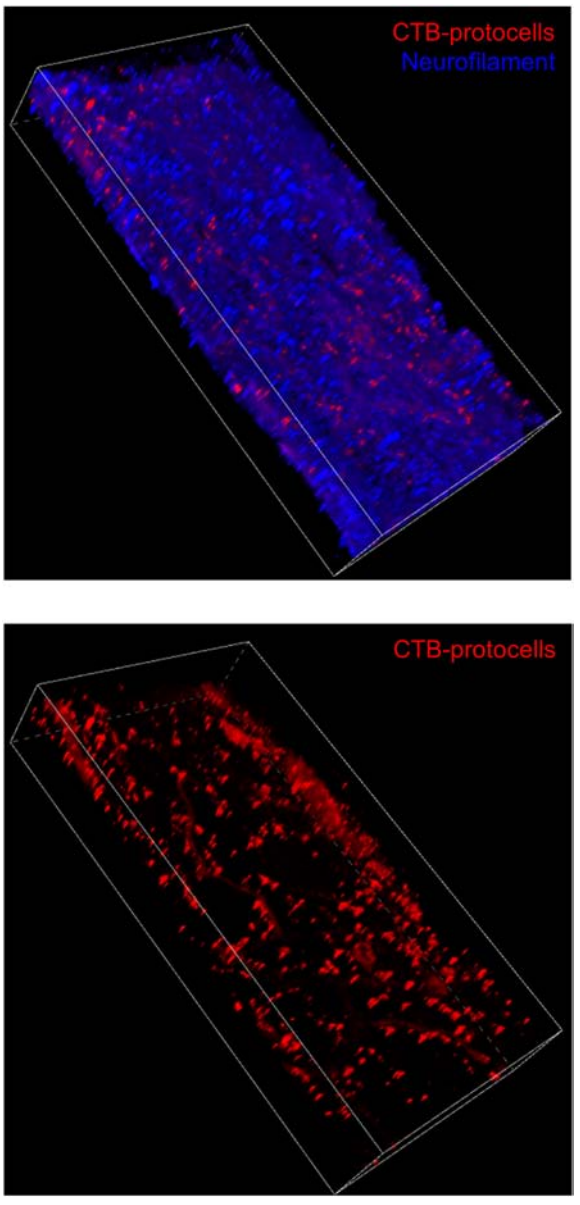

Figure 8. Evidence of CTB-protocell fluorescence after intrapleural injections. Representative 3D reconstruction of a phrenic nerve (axons labeled with neurofilament; blue) from an animal injected with CTB-protocells (n = 3 animals). CTB-protocells (red) were evident throughout the entire confocal stack.

to target the Golgi complex and regulate Golgi fragmentation in motoneurons with neurodegenerative diseases.[52] Also, TEM images showed a large portion of CTB-protocells free in the cytosol, thus CTB-protocells could also serve as a delivery platform to target cell membrane impermeable cargoes that will be available when delivered to the cytosol and that don't need to be activated by trafficking to specific organelles (e.g., lysosomes if activated at low pH). Change in incubation time did not influence localization of CTB-protocells which suggests that the binding of CTB-protocells to the plasma membrane is a fast process (<1 h), but the internalization mechanism is a continuous process that could be regulated by the frequency of the different endocytic pathways. For instance, lipid rafts associated with caveolae (mechanism for cholera endocytosis) are usually small in size and slowly internalized,[53] while macropinosomes are relatively large constituting an efficient route for the nonselective endocytosis of solutes from the extracellular fluid. CTB-protocell exocytosis was shown to be a slow process consistent with intracellular trafficking subsequent to internalization via macropinocytosis and lipid rafts. Indeed, CTB-protocells trafficked to the Golgi apparatus would be expected to be trapped in secretory vesicles for longer times.[54] Furthermore, nanoparticles that translocate into the cytoplasm show reduced exocytosis compared those in an endo-lysosomal pathway.[55]

Activity dependent uptake of CTB-protocells

The dynamic exchange of the neuronal membrane occurs primarily at axon terminals and plays an important role in multiple pathways controlling cellular homeostasis, motility and survival.[56] Activity-dependent membrane cycling occurs in response to axonal discharge and the endocytic events following synaptic vesicle release depend on stimulation frequency.[15] Under low, physiological stimulation frequencies, synaptic vesicle pools are recycled back by clathrin mediated endocytosis.[14,57] The lack of activity-dependent uptake of CTB-protocells at NMJs is consistent with clathrin-mediated endocytosis not participating in CTB-protocell uptake. The nature and molecular components of other modes of synaptic vesicle recycling and the underlying mechanisms remain a matter of debate.[15] However, some studies suggest that sustained stimulations will elicit activity-dependent bulk endocytosis of extensive membrane patches.[57] The possible impact of such stimulation on CTB-protocell uptake remains undetermined. Importantly, CTB-protocell uptake at axon terminals did not affect synaptic transmission, consistent with the lack of uptake via mechanisms used for synaptic vesicle retrieval. Furthermore, the lack of non-specific effects on synaptic function and transport via retrograde axonal mechanisms provide important proof-of-principle information towards therapeutic application of CTB-protocells in motoneurons.

Understanding cell physiological properties and mechanisms by which motoneurons interact with nanoparticles will allow improving the design of drug targeting therapy. Mechanisms of CTB-protocell endocytosis (lipid raft and macropinocytosis) and the subsequent intracellular trafficking pathways are dictated by the surface motoneuron targeting ligand CTB, the size of CTB-protocells and the main endocytic pathways present in motoneurons. The localization of CTB-protocells in the cytosol and in the Golgi apparatus suggests that CTB-protocells can effectively deliver cargo intracellularly and take a "retrograde" trafficking pathway. These studies support the utility of CTB-protocells as a motoneuron targeting therapeutic platform to engage biological pathways not readily accessible with untargeted delivery methods.

Appendix A. Supplementary data

Supplementary data to this article can be found online at https://doi.org/10.1016/j.nano.2018.01.002.

References

1. Ashley CE, Carnes EC, Phillips GK, Padilla D, Durfee PN, Brown PA, et al. The targeted delivery of multicomponent cargos to cancer cells by nanoporous particle-supported lipid bilayers. *Nat Mater* 2011;**10**:389-97.
2. Tarn D, Ashley CE, Xue M, Carnes EC, Zink JI, Brinker CJ. Mesoporous silica nanoparticle nanocarriers: biofunctionality and biocompatibility. *Acc Chem Res* 2013;**46**:792-801.
3. Sun J, Jakobsson E, Wang Y, Brinker CJ. Nanoporous silica-based protocells at multiple scales for designs of life and nanomedicine. *Life (Basel)* 2015;**5**:214-29.
4. Butler KS, Durfee PN, Theron C, Ashley CE, Carnes EC, Brinker CJ. Protocells: modular mesoporous silica nanoparticle-supported lipid bilayers for drug delivery. *Small* 2016;**12**:2173-85.
5. Gonzalez Porras MA, Durfee PN, Gregory AM, Sieck GC, Brinker CJ, Mantilla CB. A novel approach for targeted delivery to motoneurons using cholera toxin-B modified protocells. *J Neurosci Methods* 2016;**273**:160-74.
6. Zhang S, Gao H, Bao G. Physical principles of nanoparticle cellular endocytosis. *ACS Nano* 2015;**9**:8655-71.
7. Herd H, Daum N, Jones AT, Huwer H, Ghandehari H, Lehr CM. Nanoparticle geometry and surface orientation influence mode of cellular uptake. *ACS Nano* 2013;**7**:1961-73.
8. Xiang S, Tong H, Shi Q, Fernandes JC, Jin T, Dai K, et al. Uptake mechanisms of non-viral gene delivery. *J Control Release* 2012;**158**:371-8.
9. Silverstein SC, Steinman RM, Cohn ZA. Endocytosis. *Annu Rev Biochem* 1977;**46**:669-722.
10. Beddoes CM, Case CP, Briscoe WH. Understanding nanoparticle cellular entry: a physicochemical perspective. *Adv Colloid Interface Sci* 2015;**218**:48-68.
11. Chinnapen DJ, Chinnapen H, Saslowsky D, Lencer WI. Rafting with cholera toxin: endocytosis and trafficking from plasma membrane to ER. *FEMS Microbiol Lett* 2007;**266**:129-37.
12. Dietrich C, Yang B, Fujiwara T, Kusumi A, Jacobson K. Relationship of lipid rafts to transient confinement zones detected by single particle tracking. *Biophys J* 2002;**82**:274-84.
13. Zeineddine R, Yerbury JJ. The role of macropinocytosis in the propagation of protein aggregation associated with neurodegenerative diseases. *Front Physiol* 2015;**6**.
14. Royle SJ, Lagnado L. Endocytosis at the synaptic terminal. *J Physiol Lond* 2003;**553**:345-55.
15. Soykan T, Maritzen T, Haucke V. Modes and mechanisms of synaptic vesicle recycling. *Curr Opin Neurobiol* 2016;**39**:17-23.
16. Shen DK, Yang JP, Li XM, Zhou L, Zhang RY, Li W, et al. Biphase stratification approach to three-dimensional dendritic biodegradable mesoporous silica nanospheres. *Nano Lett* 2014;**14**:923-32.
17. Wang JZ, Sugawara-Narutaki A, Shimojima A, Okubo T. Biphasic synthesis of colloidal mesoporous silica nanoparticles using primary amine catalysts. *J Colloid Interface Sci* 2012;**385**:41-7.
18. Durfee PN, Lin YS, Dunphy DR, Muniz AJ, Butler KS, Humphrey KR, et al. Mesoporous silica nanoparticle-supported lipid bilayers (protocells) for active targeting and delivery to individual leukemia cells. *ACS Nano* 2016;**10**:8325-45.
19. Richard JP, Melikov K, Vives E, Ramos C, Verbeure B, Gait MJ, et al. Cell-penetrating peptides. A reevaluation of the mechanism of cellular uptake. *J Biol Chem* 2003;**278**:585-90.
20. Mantilla CB, Zhan WZ, Sieck GC. Neurotrophins improve neuromuscular transmission in the adult rat diaphragm. *Muscle Nerve* 2004;**29**:381-6.
21. Fournier M, Alula M, Sieck GC. Neuromuscular transmission failure during postnatal development. *Neurosci Lett* 1991;**125**:34-6.
22. Mantilla CB, Zhan WZ, Sieck GC. Retrograde labeling of phrenic motoneurons by intrapleural injection. *J Neurosci Methods* 2009;**182**:244-9.
23. Saraste J, Palade GE, Farquhar MG. Temperature-sensitive steps in the transport of secretory proteins through the Golgi-complex in exocrine pancreatic-cells. *Proc Natl Acad Sci U S A* 1986;**83**:6425-9.
24. Svitkina TM, Neyfakh AA, Bershadsky AD. Actin cytoskeleton of spread fibroblasts appears to assemble at the cell edges. *J Cell Sci* 1986;**82**:235-48.
25. West MA, Bretscher MS, Watts C. Distinct endocytotic pathways in epidermal growth factor-stimulated human carcinoma A431 cells. *J Cell Biol* 1989;**109**:2731-9.
26. Kilsdonk EPC, Yancey PG, Stoudt GW, Bangerter FW, Johnson WJ, Phillips MC, et al. Cellular cholesterol efflux mediated by cyclodextrins. *J Biol Chem* 1995;**270**:17250-6.
27. Motley A, Bright NA, Seaman MN, Robinson MS. Clathrin-mediated endocytosis in AP-2-depleted cells. *J Cell Biol* 2003;**162**:909-18.
28. Meier O, Boucke K, Hammer SV, Keller S, Stidwill RP, Hemmi S, et al. Adenovirus triggers macropinocytosis and endosomal leakage together with its clathrin-mediated uptake. *J Cell Biol* 2002;**158**:1119-31.
29. Wilson BS, Steinberg SL, Liederman K, Pfeiffer JR, Surviladze Z, Zhang J, et al. Markers for detergent-resistant lipid rafts occupy distinct and dynamic domains in native membranes. *Mol Biol Cell* 2004;**15**:2580-92.
30. He Q, Zhang Z, Gao F, Li Y, Shi J. In vivo biodistribution and urinary excretion of mesoporous silica nanoparticles: effects of particle size and PEGylation. *Small* 2011;**7**:271-80.
31. Teng HB, Lin MY, Wilkinson RS. Macroendocytosis and endosome processing in snake motor boutons. *J Physiol Lond* 2007;**582**:243-62.
32. Edupuganti OP, Ovsepian SV, Wang J, Zurawski TH, Schmidt JJ, Smith L, et al. Targeted delivery into motor nerve terminals of inhibitors for SNARE-cleaving proteases via liposomes coupled to an atoxic botulinum neurotoxin. *FEBS J* 2012;**279**:2555-67.
33. Lee S, Ashizawa AT, Kim KS, Falk DJ, Notterpek L. Liposomes to target peripheral neurons and Schwann cells. *PLoS One* 2013;**8**:e78724.
34. Maier O, Bohm J, Dahm M, Bruck S, Beyer C, Johann S. Differentiated NSC-34 motoneuron-like cells as experimental model for cholinergic neurodegeneration. *Neurochem Int* 2013;**62**:1029-38.
35. Matusica D, Fenech MP, Rogers ML, Rush RA. Characterization and use of the NSC-34 cell line for study of neurotrophin receptor trafficking. *J Neurosci Res* 2008;**86**:553-65.
36. Alisky JM, van de Wetering CI, Davidson BL. Widespread dispersal of cholera toxin subunit b to brain and spinal cord neurons following systemic delivery. *Exp Neurol* 2002;**178**:139-46.
37. Cartiera MS, Johnson KM, Rajendran V, Caplan MJ, Saltzman WM. The uptake and intracellular fate of PLGA nanoparticles in epithelial cells. *Biomaterials* 2009;**30**:2790-8.
38. Kang J, Heart E, Sung CK. Effects of cellular ATP depletion on glucose transport and insulin signaling in 3T3-L1 adipocytes. *Am J Physiol Endocrinol Metab* 2001;**280**:E428-35.
39. Miller CE, Majewski J, Faller R, Satija S, Kuhl TL. Cholera toxin assault on lipid monolayers containing ganglioside GM1. *Biophys J* 2004;**86**:3700-8.
40. Rodal SK, Skretting G, Garred O, Vilhardt F, van Deurs B, Sandvig K. Extraction of cholesterol with methyl-beta-cyclodextrin perturbs formation of clathrin-coated endocytic vesicles. *Mol Biol Cell* 1999;**10**:961-74.
41. Kolpak AL, Jiang J, Guo D, Standley C, Bellve K, Fogarty K, et al. Negative guidance factor-induced macropinocytosis in the growth cone plays a critical role in repulsive axon turning. *J Neurosci* 2009;**29**:10488-98.
42. Hollidge BS, Nedelsky NB, Salzano MV, Fraser JW, Gonzalez-Scarano F, Soldan SS. Orthobunyavirus entry into neurons and other mammalian cells occurs via clathrin-mediated endocytosis and requires trafficking into early endosomes. *J Virol* 2012;**86**:7988-8001.
43. Mao M, Wang L, Chang CC, Rothenberg KE, Huang J, Wang Y, et al. Involvement of a Rac1-dependent macropinocytosis pathway in plasmid DNA delivery by electrotransfection. *Mol Ther* 2017;**25**:803-15.
44. Grinstein S, Rotin D, Mason MJ. Na+/H+ exchange and growth factor-induced cytosolic Ph changes — role in cellular proliferation. *Biochim Biophys Acta* 1989;**988**:73-97.
45. Vercauteren D, Vandenbroucke RE, Jones AT, Rejman J, Demeester J, De Smedt SC, et al. The use of inhibitors to study endocytic pathways of gene carriers: optimization and pitfalls. *Mol Ther* 2010;**18**:561-9.

46. Barnakov AN. Sequential treatment by phosphotungstic acid and uranyl acetate enhances the adherence of lipid-membranes and membrane-proteins to hydrophobic EM grids. *J Microsc (Oxford)* 1994;**175**:171-4.
47. Meier O, Greber UF. Adenovirus endocytosis. *J Gene Med* 2003;**5**:451-62.
48. Wadia JS, Stan RV, Dowdy SF. Transducible TAT-HA fusogenic peptide enhances escape of TAT-fusion proteins after lipid raft macropinocytosis. *Nat Med* 2004;**10**:310-5.
49. Diaz-Rohrer B, Levental KR, Levental I. Rafting through traffic: membrane domains in cellular logistics. *BBA-Biomembranes* 1838;**2014**:3003-13.
50. Thayer DA, Jan YN, Jan LY. Increased neuronal activity fragments the Golgi complex. *Proc Natl Acad Sci U S A* 2013;**110**:1482-7.
51. Ferrari A, Pellegrini V, Arcangeli C, Fittipaldi A, Giacca M, Beltram F. Caveolae-mediated internalization of extracellular HIV-1 tat fusion proteins visualized in real time. *Mol Ther* 2003;**8**:284-94.
52. Liu C, Mei M, Li Q, Roboti P, Pang Q, Ying Z, et al. Loss of the golgin GM130 causes Golgi disruption, Purkinje neuron loss, and ataxia in mice. *Proc Natl Acad Sci U S A* 2017;**114**:346-51.
53. Conner SD, Schmid SL. Regulated portals of entry into the cell. *Nature* 2003;**422**:37-44.
54. Sakhtianchi R, Minchin RF, Lee KB, Alkilany AM, Serpooshan V, Mahmoudi M. Exocytosis of nanoparticles from cells: role in cellular retention and toxicity. *Adv Colloid Interface Sci* 2013(201-202):18-29.
55. Stayton I, Winiarz J, Shannon K, Ma YF. Study of uptake and loss of silica nanoparticles in living human lung epithelial cells at single cell level. *Anal Bioanal Chem* 2009;**394**:1595-608.
56. Deinhardt K, Schiavo G. Endocytosis and retrograde axonal traffic in motor neurons. *Biochem Soc Symp* 2005;**72**:139-50.
57. Clayton EL, Cousin MA. Quantitative monitoring of activity-dependent bulk endocytosis of synaptic vesicle membrane by fluorescent dextran imaging. *J Neurosci Methods* 2009;**185**:76-81.